Narrowband Metamaterial Absorber for Terahertz Secure Labeling

Magued Nasr [*a], Jonathan T. Richard [*d], Scott A. Skirlo [*b], Martin S. Heimbeck [c], John D. Joannopoulos,[b] Marin Soljacic [b], Henry O. Everitt [c†], Lawrence Domash [a]

[*] Equal contributors

[a] Triton Systems Inc., 200 Turnpike Rd #2, Chelmsford, MA 01824

[b] Department of Physics, Massachusetts Institute of Technology, Cambridge, MA 02139

[c] U.S. Army Aviation and Missile RD&E Center, Redstone Arsenal, AL 35898

[d] IERUS Technologies, 2904 Westcorp Blvd Suite 210, Huntsville, AL 35805

† Corresponding author: henry.o.everitt.civ@mail.mil

Abstract

Flexible metamaterial films, fabricated by photolithography on a thin copper-backed polyimide substrate, are used to mark or barcode objects securely. The films are characterized by continuous wave terahertz spectroscopic ellipsometry and visualized by a scanning confocal imager coupled to a vector network analyzer that constructed a terahertz spectral hypercube. These films exhibit a strong, narrowband, polarization- and angle-insensitive absorption at wavelengths near one millimeter. Consequently, the films are nearly indistinguishable at visible or infrared wavelengths and may be easily observed by terahertz imaging only at the resonance frequency of the film.

Introduction

Terahertz radiation in the long wavelength 1 - 3 mm band penetrates dry dielectrics such as plastics, concrete, and fabric while being strongly absorbed by water and water vapor. This combination of characteristics may be exploited for numerous applications including short-range communications and radar, collision avoidance radar, non-destructive testing of materials and structures, security imaging, medical diagnosis, and spectroscopy.[1,2,3] Materials with interesting terahertz properties also play a role in numerous security applications due to their limited range and high bandwidth. One potential use could be to encode markings, signs, or barcodes on objects, such as railway cars or shipping containers that are invisible to the unaided human eye but can be read at high speed by narrowband scanning terahertz imaging systems operating at the correct frequency. Radio frequency identification (RFID) techniques can also provide such information but cannot be used for certain applications, such as when RF power must be limited (e.g. for containers containing explosives, strong co-site interference, or covert interrogation) or imaging is required. Here, we demonstrate how such markings could be implemented in a thin material with a narrowband, absorptive resonance and used to write a 2D spatial pattern that is readable by a terahertz imaging system over a wide range of angles but only at a pre-specified frequency.

Thin metamaterial 'perfect absorber' structures for the terahertz region have been explored previously.[4,5,6] One basic design family uses three layers; an opaque metal backplane layer, a dielectric spacer, and a plane of periodic metal islands whose lateral size is typically on the order of 1/4 the resonant wavelength. A "perfect absorber" design is reflective over a wide band of frequencies but strongly absorptive at one resonant frequency.[7] Such designs are intrinsically omnidirectional, provided the islands are closely spaced. For a metamaterial resonant around 1 mm wavelength, the entire thickness of the three key layers can be less than 25 μm. Most previous demonstrations have been fabricated on semiconductor wafers, and some have been fabricated on flexible substrates.[8,9] Here we report a low cost approach where the substrate is a commercially available metal-coated polyimide. A single step of photolithography was sufficient to convert the substrate into a resonant metamaterial. To make larger areas, photolithography could be replaced by various electronic printing methods.[10]

Design and Fabrication

Design and fabrication of metamaterial absorbers at microwave and terahertz frequencies using the three-layer backplane-dielectric spacer-metal array format have been extensively described.[8,11,12,13] In the layer containing an array of metal islands, a variety of patterns such as rings, split-rings, or cut wires can be used to create resonances. Tuning the geometrical parameters of a given design changes the effective permeability and permittivity of the metamaterial and the resonant frequency. The quality of the absorber is determined by how closely the impedance of the metamaterial matches free-space and by the magnitude of the imaginary parts of μ and ε at resonance.

The goal was to design and fabricate a flexible metamaterial film with strong absorption near 0.3 THz (~1 mm wavelength), building on a commercially available substrate. For ease of fabrication and to ensure line widths are constant throughout, a pattern of square rings was selected that contained no extremely small features (< 2 microns) that might lead to manufacturing errors.[8,14] DuPont's flexible electronic material Pyralux® LF7012R,[15] a copper-clad polyimide laminate made from a 12.7 µm film of Kapton with a 17.4 µm copper backing, was used to support these square rings. This composite has low loss, precise thickness, maintains the mechanical strength of the constituent materials, and has successfully been used previously to fabricate metamaterial absorbers.[9]

To design a panel with a narrowband, polarization-independent response over the widest possible field of view, the commercial electromagnetic solver Microwave CST was used, simulating the normal-incidence and large-angle absorption of the metamaterial for TE and TM polarizations. The simulation consisted of a single cell of the metamaterial with periodic boundary conditions for the in-plane directions. CST solved the transmission and reflection of the structure using a frequency domain form of the finite-integration technique, which is similar to the FDFD (finite-difference frequency-domain) method.

The resonance frequency of the absorber is sensitive to the lateral dimensions of the square rings, whereas the magnitude of the absorption depended mostly on the conductivity and thickness of the upper metal layer, since the spacer layer is fixed. This behavior is expected as the lateral dimensions of the upper layer determine the effective inductance and capacitance of the resonator, while the conductivity and thickness affect the resistance. The capacitive part of the resonator originates from the gaps between the neighboring metal rings, and the separation between the metal backplane and the rings.[16] The gaps between the rings were made large in the final design to minimize the error from this capacitance since it had the poorest tolerance for lateral dimensions. The inductive part of the resonance is controlled by the width and perimeter of the rings themselves.

Figure 1a shows two of the unit cell layouts investigated. Design A consisted of a hollow square about 190 μm in size, repeated on a 240 μm pitch, with a feature linewidth of about 20 μm, for a predicted center frequency of 285 GHz. In Design B the dimension for the hollow square was reduced to 170 μm while keeping the pitch constant to produce a higher resonant frequency near 320 GHz. A higher resonance frequency was expected for this design because the perimeter of the square ring is reduced, reducing the inductance of the ring and the capacitance with the backplane. From these arguments the new resonance frequency was expected to be roughly [(190 μm/170 μm) x 285 GHz] = 319 GHz, which matches the simulations fairly well.

We simulated, fabricated, and measured a number of such designs to investigate how varying these parameters affected the resonance frequency and absorption. The hollow square pattern was fabricated using photolithography, sputtering 10 nm of Cr on the Kapton followed by 500 nm of Au. Figure 1b is a photograph of one of the samples following the photolithographic patterning of the Cr/Au layer on the Kapton-copper substrate. The metamaterial structure is too small to be resolved by unaided eye, but is revealed in the photomicrographs. (Figs. 1c, d). Calculated reflectivity spectra for Design A reveal that the resonance frequency and absorption stay roughly the same as a function of angle for both TE and TM polarizations.

Although perfect omnidirectional performance is not possible, samples can be designed to be relatively insensitive to a broad range of incidence angles away from normal. The reflection parameter S_{11} for a PEC backed absorber for a TE-polarized mode can be written as[17]

$$S_{11} = \left[\frac{-k_z\ \cos k_z L - i\mu_{xx}\, k_0 \cos\theta \sin k_z L}{k_z\ \cos k_z L - i\mu_{xx}\, k_0 \cos\theta \sin k_z L}\right] e^{-i2k_0 \cos k_z L}, \qquad [1]$$

where $k_z = k_0\sqrt{\epsilon_{yy}\mu_{xx} - \ \mu_{xx}(sin\theta)^2/h}$, θ is the angle of incidence, $\mu_{xx}(\omega)$ is the x-component of the permeability, $\epsilon_{yy}(\omega)$ is the y-component of the permittivity, h is z-component of the permeability, and L is the absorber thickness. These material parameters can be extracted from the transmission and reflection coefficients experimentally or from the metamaterial cell simulation. When $\epsilon(\omega) = \mu(\omega) = \alpha + i\alpha'$, for large α', S_{11} shrinks rapidly with increasing L because the metamaterial is simultaneously impedance matched to free space and strongly absorptive.

Although S_{11} is minimized under these conditions at $\theta = 0$, for $\theta \neq 0$ the resonance frequency and Q of the absorber will shift, an effect that has been seen in other optimized metamaterial absorbers.[8,15] Therefore, we optimized at normal incidence recognizing that the reflection coefficient correction for non-normal incidence is small and decreases as $(1-\theta^2)$. Consequently, off-axis absorption maintains a relatively constant resonance frequency and Q over a wide range of incidence angles.[8,15] Figure 2, which plots the normalized reflection for Design A as a function of incident angle and polarization, demonstrates the relative insensitivity of the signature to incidence angle up to ±60° for TM polarization and ±40° for TE polarization. For the TM polarization, the magnetic field maintains the same magnitude over these angles, whereas for TE the induced magnetization falls off, causing degradation in the impedance matching and decreasing the Q.[8]

Measurement

The films were analyzed in a reflection geometry using a Woollam terahertz spectroscopic ellipsometer that measured the polarization-dependent change in amplitude and phase induced by the dielectric properties of the sample when the frequency-scanned terahertz beam reflected from its surface.[18] The terahertz ellipsometer generated incident radiation using a frequency tunable backward wave oscillator and frequency multiplier, then recorded the reflected parallel and vertical polarized terahertz signal over a range of 220 – 330 GHz, as shown in Figure 3. The samples' spectral reflectivities were estimated by referencing the raw metamaterial signal to reflection measurements using a bulk aluminum mirror. Since resonance frequency is nearly independent of angle of incidence and polarization near normal incidence, the measurements were taken for angles of incidence away from normal to explore the sensitivity of the signatures to the angle of incidence.

The data confirmed all the predicted behaviors of the resonance feature: the slight blueshift of the center frequency and the polarization-dependent slow increase of line width as the angle of incidence increased. The absorption peak at 292 GHz for Design A was only slightly higher than the predicted frequency. Although the absorption peak could not be observed for Design B because of the limited spectral coverage of the ellipsometer, an absorption tail was visible at the upper end of the frequency range, suggesting this peak was also slightly higher than the predicted frequency. The small discrepancy between the calculated and measured resonant frequencies and linewidths likely originates from the uncertainty associated with the dielectric constant of Kapton and manufacturing imperfections. The dielectric constant used for Kapton in the original simulations was $\varepsilon = 3.37 + 0.039i$.[19] However, the simulations showed the best agreement with experiment using a dielectric constant of $3.5 + 0.007i$, a value consistent with other measurements performed at 60 GHz.[20] Small fabrication errors, such as the rounding of corners, also broadened the absorption peak and shifted its frequency.

Rozanov discovered a relationship between the absorption-bandwidth product and the absorber thickness, an observation that can be used to estimate how close our absorbers are to optimal.[21,22] Applying this to normal incidence simulations for Design A, the minimum thickness for any absorber design reaching the same absorbance performance is 7.6 μm. This is not much less than the 12.7 μm total thickness of the actual absorber, implying that the design is close to optimal.

Secure Labeling

To demonstrate the secure labeling concept, 1 cm wide strips of the Design A material were bonded on a sheet of unstructured Pyralux film to form a letter "A" about 15 cm high. The resulting sample was about 20 x 15 cm in area, and the metamaterial tape against the Pyralux background was nearly invisible to the unaided eye (Figure 1b). The strips were affixed with ordinary packaging tape, raising the refractive index of the medium surrounding the metamaterial and red shifting the resonance frequency from near 290 GHz to near 250 GHz. The expected decrease may be estimated assuming a refractive index for the tape of about 1.7,[23] and simulations adding this external index produced a shift in resonance frequency close to the observed value. Other local changes in the dielectric environment, such as delaminations of the host material or the accretion of environmental adsorbates, will also slightly shift the resonance away from the design frequency. Although the spectrometer may have to sample nearby frequencies to locate the resonance, this could represent another advantage of the technique, as it detects changes in local conditions that may signal deterioration of the structure while preserving the narrow linewidth that prevents accidental or malicious detection.

To observe this “invisible A”, a terahertz confocal imager system was constructed from a Virginia Diodes G-band transceiver, which served as a frequency extender to an Agilent 5222A vector network analyzer (VNA). Specifically, the VNA provided the local oscillator (LO) and fundamental 10 – 20 GHz transmit signal (RF) for the Virginia Diodes 220 – 330 GHz transceiver. The LO and RF arrive at the transceiver input with a frequency offset of 279 MHz. The transceiver’s internal hardware multiplies the LO and

RF signals by a factor of 18 to produce an RF output of 220 – 330 GHz and an LO of 219.721 – 329.721 GHz. The LO is mixed with the reflected RF signal, producing a 270 MHz intermediate frequency (IF) that was processed by the VNA to record amplitude and phase information in I and Q format.

The transceiver used a collimating lens followed by a second lens to focus the THz beam and interrogate a 2 mm diameter circular region of the sample, which is the smallest resolvable spot or "pixel". At each pixel location, the frequency was swept from 220 to 330 GHz, and the VNA receiver referenced the measured reflected signal to the transmitted signal. Reflected signals were sampled at 1601 different frequencies, representing a frequency resolution of 68.7 MHz. These measurements were then combined into a single image using a two-dimensional raster scan of 100 vertical pixels by 75 horizontal pixels on a 2 mm pitch to minimize acquisition time without sacrificing resolution.

After the data was collected for each pixel, a wide range gate was applied through post-processing to eliminate spurious signals, isolate the object, and plot the terahertz spectral hypercube. To accomplish this range gate, an inverse fast Fourier transform (IFFT) was first applied to the measured frequency-domain data of each pixel to generate the complementary time-domain (i.e. range-domain) signature from which the return range of the sample was obtained. The sample was then range isolated by setting to -120 dB all range bins ±11 cm beyond the target. (The noise floor itself spanned -70 to -90 dB, while the target reflection reached -30 dB.) After applying a planar interpolation to compensate for non-normal placement of the sample, an FFT was applied to the remaining range domain data to produce a spectrum.

This spectrum represents a single pixel, a vertical column in the terahertz hypercube, four of which are plotted in Figure 4. Because of the contrast-enhancement and phase sensitivity of our imaging technique, the images show a pattern of changes in absorption that are visible over about a 40 GHz bandwidth, consistent with the >30 GHz width over which the absorption feature seen in Figure 3 is reduced at least 3 dB. Horizontal planar slices through the terahertz hypercube produce spectrally resolved images, and five are also shown around the periphery of Figure 4. A "movie" of these images, sweeping through the hyperplanes one frequency at a time, can be viewed in the supplemental material. The metamaterial tape is most clearly visible over a narrow, 3.25 GHz FWHM absorptive band near 250.2 GHz with >15 dB of attenuation. Averaging up to 15 hyperimages, and thereby reducing spectral resolution to 1 GHz, did not significantly improve the image quality. This suggests excellent uniformity in size and shape of the constituent metamaterials throughout the panel.

Discussion

In this demonstration we used strips of patterned material bonded onto unpatterned material. The demonstration of secure labeling presented here could be improved if, instead of a single frequency tape over an unstructured background, two or more different patterns with different metamaterial resonances were used, distributed over an area to form a spatial pattern representing characters or barcodes. Two slightly different metamaterial designs, with different resonant frequencies for the two subareas of characters and background, would be even harder to detect by inspection. These could be fabricated by single combined step of photolithography or printing.

Heterogeneous metamaterials with different resonant frequencies would then correspond to different spatial patterns at different spectral layers in the terahertz hypercube. By using two or more tapes with different resonant frequencies, the inscribed characters or message would change depending on the frequency of illumination. In this way, a movie of sorts could be encoded in the metamaterial structure that could be played simply by scanning the interrogating frequency. Within the moderate resolutions used here, larger areas of metamaterial film could easily be produced by screen printing with metallic inks or using other electronic printing methods.

In addition to secure labeling, these structures may be configured as sensors since the resonant frequencies of the metamaterials depend on local environmental conditions such as strain, moisture, or damage. Notice that the resonance frequency shifted approximately 40 GHz, more than a dozen linewidths, by the simple application of transparent packing tape over the metamaterial surface, indicating a strong sensitivity to the local dielectric environment. Similarly, embedded metamaterial panels would represent a novel technique for structural monitoring of delamination, cracks in concrete, and incipient mechanical failure. Such an adaptation represents a step beyond passive radio frequency identification (RFID) techniques by exploiting the superior resolution of terahertz probes to provide spatially resolved status information from a target of interest. This opportunity is further enhanced by the comparatively strong attenuation provided by the atmosphere, limiting the problems posed by multi-site interference and constraining the propagation range of the interrogating terahertz beam. This technique will be best applied over short-ranges (< 1 km) and could provide significant advantages when interrogating materials that may be sensitive to the much stronger electromagnetic signals typical of RFID interrogation scans.

Conclusion

We have demonstrated a simple method for making signage, barcodes, or sensors which are nearly invisible to the naked eye or IR imagers but can be easily read by scanning or imaging at a specific frequency in the terahertz range. Such materials appear manufacturable in large areas with metal printing techniques for application to security, the shipping industry, or structural monitoring.

Acknowledgements

This work was supported the US Army Institute for Soldier Nanoscience at the Massachusetts Institute of Technology and Triton Systems Internal Research and Development Program 1500-197. The authors wish to thank John Blum for his contributions to alternative fabrication methodologies.

Supporting Information

A video version of the terahertz hypercube images, sweeping through the hyperplanes one frequency at a time, can be viewed in the supplement.

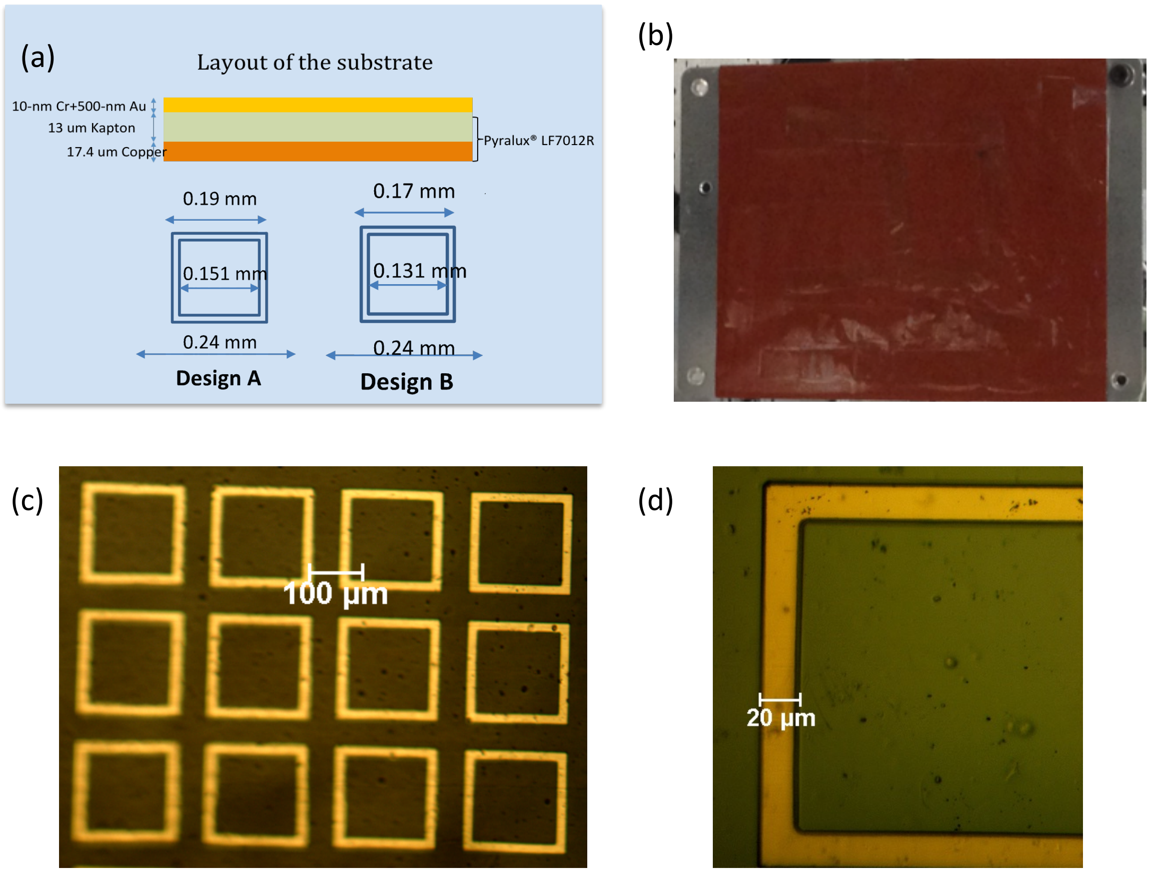

Figure 1. (a) Two designs for resonant frequencies of 285 GHz (Design A) and 320 GHz (Design B). (b) Photograph of the secure labeling sample, made from strips of Design A metamaterial bonded onto unstructured Pyralux. The pattern is nearly invisible to the eye. (c-d) Metamaterial film after photolithography, shown at two different magnifications.

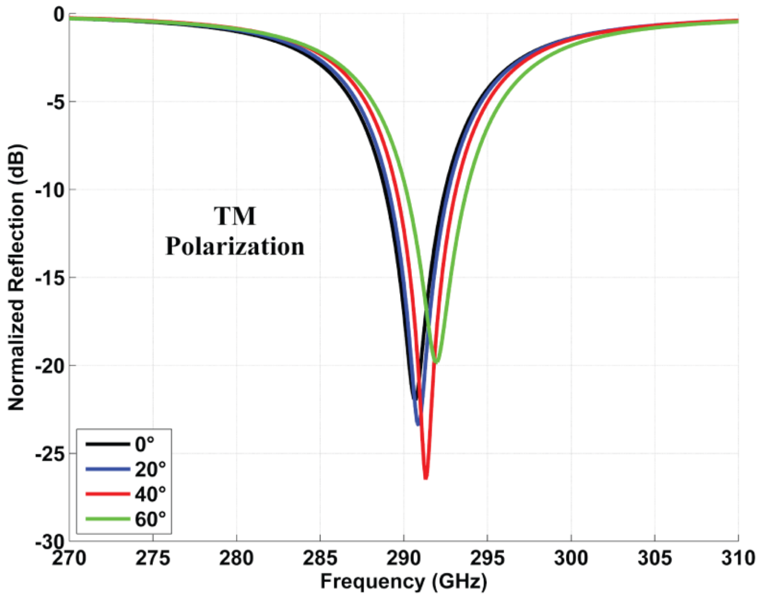

Figure 2. Normalized reflection for Design A, plotted as a function of incident angle and polarization, revealing the degree of insensitivity to these parameters.

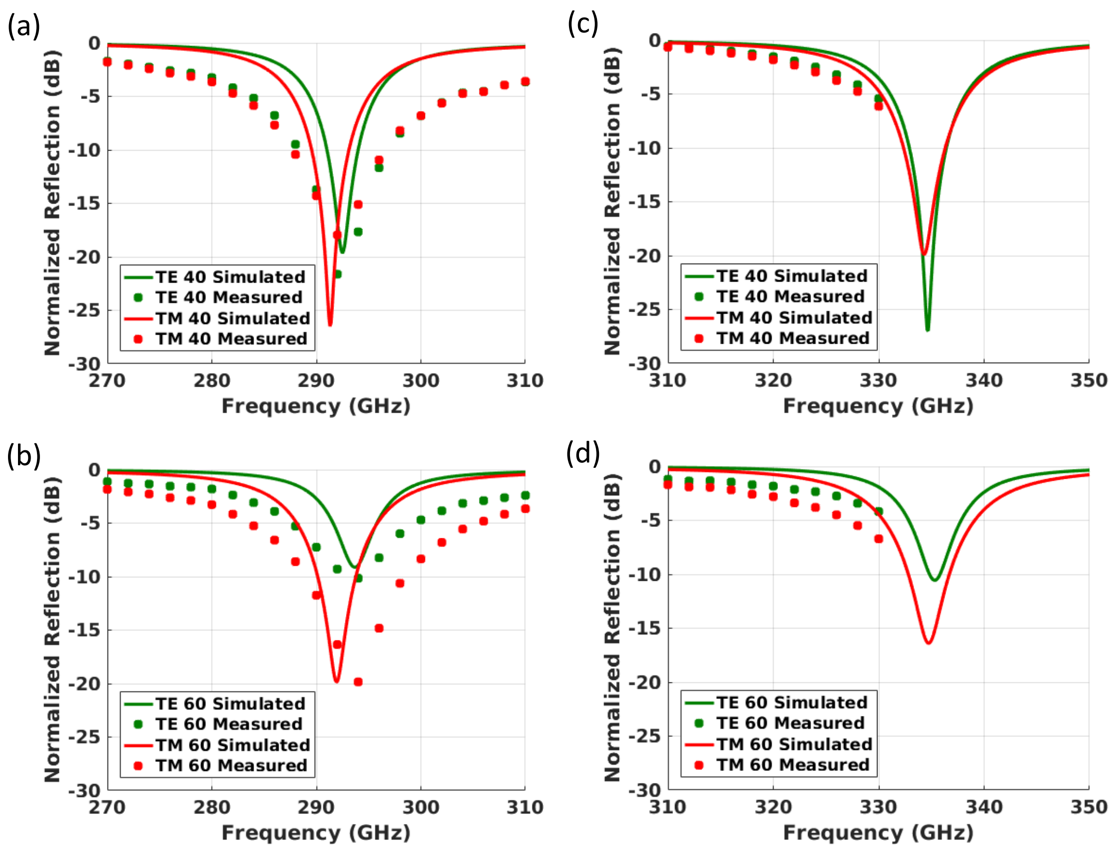

Figure 3. The reflectance spectra of Designs A (a,b) and B (c,d), measured using the terahertz ellipsometer for incidence angles of 40° (a,c) or 60° (b,d) and both linear polarizations, compared with the corresponding calculations.

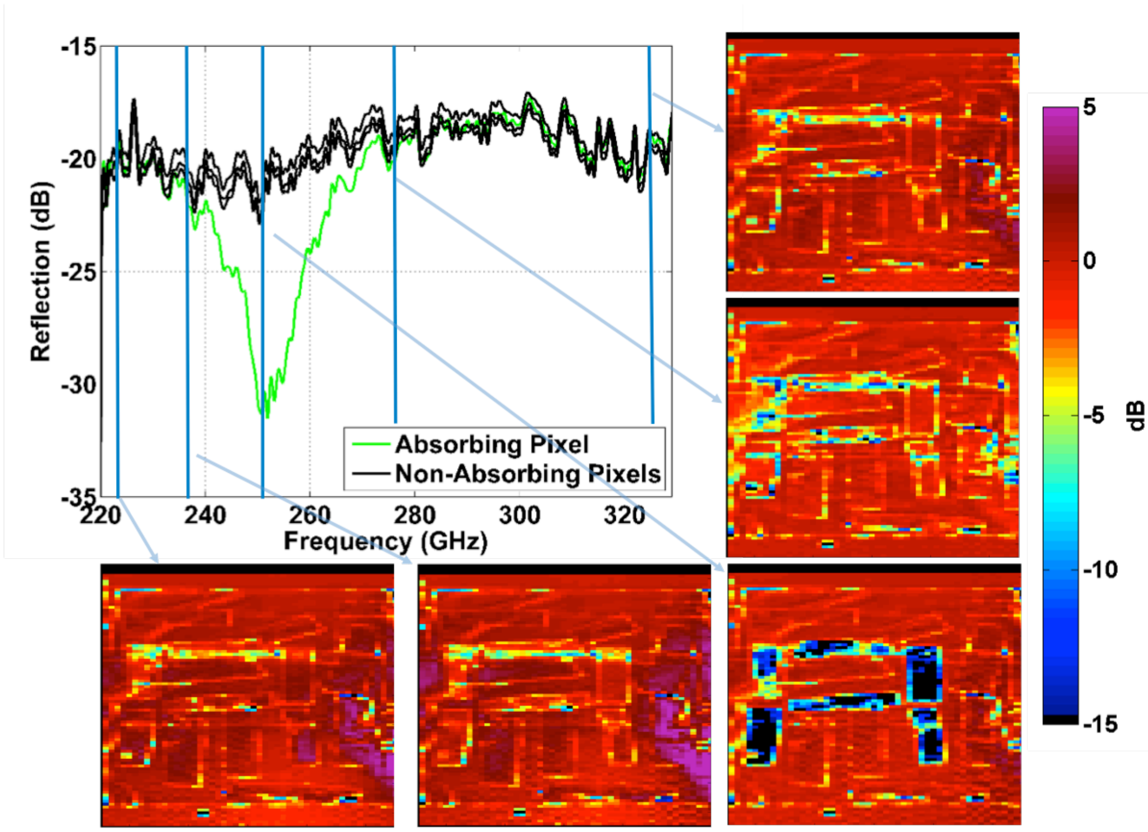

Figure 4. Spectra of four pixels, one of which is located on the metamaterial region, and five normalized, range-gated 2D terahertz hyperplane images at (from left to right and bottom to top) 233, 237, 251, 278, and 326 GHz. The image of the letter A is seen most clearly near 251 GHz. The supplement contains a video of the full terahertz spectral hypercube.

References

[1] P. Siegel, "THz Technology: An Overview", *Terahertz Sensing Technology. Volume 1: Electronic Devices and Advanced Systems Technology*, pp. 1–44, World Scientific, Singapore, 2003.

[2] D. Mittleman, *Sensing with Terahertz Radiation,* Springer, New York, 2003.

[3] H.O. Everitt and F.C. De Lucia, "Detection and Recognition of Explosives using Terahertz-Frequency Spectroscopic Techniques," *Laser-Based Optical Detection of Explosives*, CRC Press, Taylor & Francis Group, Boca Raton, 2015.

[4] H-T Chen, W. J. Padilla, J. M. O. Zide, A. C. Gossard, A. J. Taylor, and R. D. Averitt, "Active terahertz metamaterial devices", *Nature* **2006**, *444*, 597-600.

[5] H-T Chen, W. J. Padilla, R. D. Averitt, A. C. Gossard, C. Highstrete, M. Lee, J. F. O'Hara, and A. J. Taylor, "Electromagnetic Metamaterials for THz Applications," *Terahertz Science and Technology* **2008**, *1* (1), 42-50.

[6] N. I. Landy, C. M. Bingham, T. Tyler, N. Jokerst, D. R. Smith, and W. J. Padilla, "Design, theory and measurement of a polarization-insensitive absorber for terahertz imaging," *Phys. Rev. B* **2009,** *79*, 125104.

[7] M. Diem, T. Koschny, and C. M. Soukoulis, "Wide-angle perfect absorber/thermal emitter in the terahertz regime," *Phys. Rev. B* **2009**, *79*, 033101.

[8] H. Tao, C. M. Bingham, A. C. Strikwerda, D. Pilon, D. Shrekenhamer, N. I. Landy, K. Fan, X. Zhang, W. J. Padilla, and R. D. Averitt, "Highly flexible wide angle of incidence

terahertz metamaterial absorber: Design, fabrication, and characterization," *Phys. Rev. B* **2008,** *78* (24), 241103.

[9] M. Walther, A. Ortner, H. Meier, U. Löffelmann, P. J. Smith, and J. G. Korvink, "Terahertz metamaterials fabricated by inkjet printing," *Appl. Phys. Lett.* **2009**, *95* (25), 251107.

[10] X. Liu, M. Kanehara, C. Liu, K. Sakamoto, T. Yasuda, J. Takeya, T. Minari, "Spontaneous Patterning of High-Resolution Electronics via Parallel Vacuum Ultraviolet," *Adv. Mat.* **2016**, *28* (31), 6568-6573.

[11] Y. Ra'di, C. R. Simovski, and S. A. Tretyakov, "Thin Perfect Absorbers for Electromagnetic Waves: Theory, Design, and Realizations," *Phys. Rev. Appl.* **2015**, *3*, 037001.

[12] J. Yang, and Z. Shen. "A thin and broadband absorber using double-square loops," *IEEE Antennas and Wireless Propagation Lett,* **2007**, *6*, 388-391.

[13] H. Kim, J. S. Melinger, A. Khachatrian, N. A. Charipar, R. C. Y. Auyeung, and A. Piqué, "Fabrication of terahertz metamaterials by laser printing", *Optics Letters* **2010**, *35* (23), pp. 4039-4041.

[14] R. Ortuño, C. García-Meca, and A. Martínez , "Terahertz Metamaterials on Flexible Polypropylene Substrate", *Plasmonics*, **2014**, *9* (5) pp. 1143-1147.

[15] http://www.insulectro.com/content_media/file/Dupont_LFclad_H-73244.pdf.

[16] J. Yang, and Z. Shen. "A thin and broadband absorber using double-square loops," *IEEE Antennas and Wireless Propagation Lett,* **2007**, *6*, 388-391.

[17] D. Ye, Z. Wang, Z. Wang, K. Xu, B. Zhang, J. Huangfu, C. Li, L. Ran, “Towards Experimental Perfectly-Matched Layers With Ultra-Thin Metamaterial Surfaces,” *IEEE Trans Antennas Prop.* **2012**, 60, 5164

[18] T. Hofmann, C. M. Herzinger, A. Boosalis, T. E. Tiwald, J. A. Woollam, and M. Schubert, “Variable-wavelength frequency-domain terahertz ellipsometry,” *Rev. Sci. Instrum.* **2010**, *81*, 023101.

[19] J. M. Lau, J. W. Fowler, T. A. Marriage, L. Page, J. Leong, E. Wishnow, R. Henry, E. Wollck, M. Halpern, D. Marsden, G. Marsden, "Millimeter-wave antireflection coating for cryogenic silicon lenses," *Appl. Opt.* **2006**, *45* (16), 3746-3751.

[20] A. Ali, M. M. Jatlaoui, S. Hebib, H. Aubert, D. Dragomirescu, "60 GHz Rectangular Patch Antennas on Flexible Substrate: Design and Experiment," *Progress In Electromagnetics Research Symposium Abstracts*, (Marrakesh, Morocco, Mar. 20-23, 2011) *Session 2P9*: Poster Session 4, 610.

[21] K. N. Rozanov, "Ultimate thickness to bandwidth ratio of radar absorbers," *IEEE Trans. on Antennas and Propagation,* **2000**, *48* (8), 1230-1234.

[22] D. Ye, Z. Wang, K. Xu, H. Li, J. Huangfu, Z. Wang, and L. Ran, "Ultrawideband dispersion control of a metamaterial surface for perfectly-matched-layer-like absorption," *Phys. Rev. Lett.* **2013**, *111***,** 187402.

[23] J. M. Woo, D. Kim, S. Hussain, and J.-H. Jang, “Low-loss flexible bilayer metamaterials in THz regime,” *Opt. Exp.* **2014**, *22* (3), 2289-2298.